

Application of the List Viterbi Algorithm for Satellite-based AIS Detection

Linda Kanaan^{1,2}, Karine Amis¹, Frédéric Guilloud¹, Rémi Chauvat³

¹ IMT Atlantique, Lab-STICC, 29238 Brest, France,

² TésA, 31000 Toulouse, France,

³ Kinéis, 31520 Ramonville Saint-Agne, France

emails: {linda.kanaan, karine.amis, frederic.guilloud}@imt-atlantique.fr, rchauvat@kineis.com

Abstract—Satellites receiving Automatic Identification System (AIS) packets in dense areas are particularly prone to AIS channel overload due to the extensive number of vessels. Thus a failure of detection might be caused by the collisions among AIS messages. To improve the detection capability, we propose to exploit the presence of the cyclic redundancy check (CRC) in AIS frames by using the parallel list Viterbi algorithm (PLVA) instead of the classical Viterbi algorithm (VA) often used for decoding AIS signals. The performance of combining the PLVA with AIS post processing including the CRC is studied with two detectors, one coherent and the other differential, in two channel models: a single-user AWGN channel and a more realistic multiple-access AIS channel. We also show the impact of the PLVA parameters on the success recovery rate. The simulation results show that the resulting procedure can significantly improve the packet error rate (PER) at the cost of a limited increase of the computational complexity. The proposed technique could be applied to improve the performance of interference cancellation receivers by significantly lowering the AIS decoding threshold.

Index Terms—

Automatic identification system (AIS), list Viterbi algorithm (LVA), packet collision, differential detector, coherent detector.

I. INTRODUCTION

AIS [1] is employed in the maritime sector to ensure vessel traffic safety. The AIS signal is generated and broadcast via standardized very high frequency (VHF) transceivers, thus allowing ships to automatically exchange information with other ships and nearby coastal stations up to 20 to 30 nautical miles.

Starting from 2007, AIS receivers have been embedded into low earth orbit (LEO) satellites (Sat-AIS) [2], enabling global supervision of the maritime traffic. Since AIS was mainly developed for terrestrial communications, the Sat-AIS reception has been accompanied by several challenges including message collisions, propagation delay, attenuation and Doppler effect. In environments with high vessel density, the likelihood of AIS message collisions increases because vessels are unable to coordinate their transmissions beyond a distance way below the footprint of the satellite, leading to a higher probability of undetected or incorrectly decoded

signals. This necessitates the implementation of highly reliable decoding mechanisms to ensure the integrity of the transmitted information.

Several approaches have been considered for mitigating the interference for AIS detection, this includes antenna array processing [3], [4], bandwidth separation in sub-zones [5] and interference cancellation approaches [6]–[8]. It is important to note here that these three approaches could be combined altogether. However, all these approaches are intrinsically limited by the poor energy efficiency of the (uncoded) AIS signals, forbidding correct decoding except for large values of received signal-to-noise plus interference ratio. Whereas previous works [9], [10] exploit a priori information on AIS message bits based upon statistical analysis and knowledge of satellite position, we assume uniformly distributed bits in this paper. However, exploiting this knowledge could be combined for further improvement.

In this paper, we intend to improve AIS decoding by generating candidates diversity (i.e. sequence diversity) with a later perspective of improving the performance of receivers including interference cancellation. The AIS frame definition constraints including the CRC will be used to ensure the validity of each candidate. Prior works have already proposed to exploit the CRC for error correction in AIS. In [5], two simple yet effective strategies are proposed, bit flipping and exploiting syndromes of CRC codewords. Both do not use the trellis structure, instead, soft demodulated outputs are exploited. In [6], maximum likelihood sequence estimation (MLSE) including CRC and bit stuffing constraints is performed. This yields the best performance in the single user approach so far, but it has significant computational complexity. To the best of our knowledge, the application of the list Viterbi algorithm (LVA) to the AIS context has not been analyzed so far. Due to the capability of LVA to maintain multiple candidate paths, researchers have been able to achieve significant advancements in accuracy and reliability in different fields. Different applications of LVA along with an outer code for error detection (typically CRC) appeared in the literature [11]–[14]. Parallel LVA (PLVA) has been proposed in [11], [12] and improved in [15]. An alternative to the PLVA

This work has been financially supported by Kinéis, CNES and Région Bretagne.

is the serial LVA (SLVA) proposed in [11], [16], [17].

As previously mentioned, our objective is to reduce the packet error rate (PER) thanks to candidates diversity. To achieve this, PLVA is implemented instead of the VA [18] for the Gaussian minimum shift keying (GMSK) demodulation. The contributions of this paper are (i) Application of PLVA for AIS signals detection in a single user AWGN channel (ii) Optimization of the PLVA parameters for the optimized coherent and differential detection of AIS signals (iii) Simulations with optimized PLVA for realistic AIS signals parameters. The remainder of this paper is organized as follows. Section II gives an overview of the AIS medium access scheme and the consequences of satellite reception. It also describes the AIS packet structure and system model. Section III presents the decoders implemented for the detection of AIS signals. This is followed by the LVA principle combined with the AIS message post-processing in Section IV. Simulation results are provided in Section V. Finally, a conclusion is drawn in Section VI.

II. SYSTEM MODEL

A. AIS access protocol

AIS is a synchronized network using time slotted access to its radio channels. Self-organized time division multiple access (SOTDMA) constitutes AIS main access scheme. Under this mode of operations, vessels are avoiding the selection of the same time slots by listening to the AIS channels and advertising in their messages the next slots they intend to use.

When the vessels are sufficiently close to each other, there is likely no collision among the transmitted signals due to the SOTDMA scheme and the differential propagation delays much inferior to the AIS buffer length located at the end of the AIS packet (see Fig. 1). However, if the AIS signals are transmitted from vessels that are far from each other within the satellite footprint, two types of collision could occur.

The signal collision due to uncoordinated transmissions targeting the same time slot in two different SOTDMA cells leads to a full collision among the signals. The interference resulting from this type of collision is denoted here "Class 1 Interference". The number of ships within satellite detection range and the rate at which ships report determine how many collisions of this kind occur during each time slot. In the case of a satellite reception with large ground footprint, the number of interfering signals can potentially be very important especially in dense maritime areas.

Furthermore, even if the network operates in a synchronous manner (i.e. with temporal slots synchronized on UTC time), the different propagation delay within signals can generate partial collisions between adjacent slots. The interference resulting from this type of collision is denoted here "Class 2 Interference". It has less impact on the decoding performance.

B. AIS packet

The ITU-R M.1371-5 standard [1] covers the description of the AIS signal format transmitted by the vessels. Briefly, an AIS packet is N bits long where $224 \leq N \leq 256$. An AIS slot has a duration of 256 AIS symbols and assuming perfect

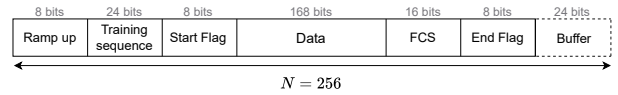


Fig. 1: AIS packet

SOTDMA, a single AIS packet should be transmitted per slot. An AIS packet contains signaling and data bits following the structure of Fig. 1.

After the transmission of the AIS data (168 bits), the cyclic redundancy check (CRC) is computed and appended in the FCS field, thus creating the data message part of the AIS packet. Bit stuffing is then performed in order to avoid long '1' sequences and the existence of the '0111110' pattern reserved for the start flag and the end flag. Afterward the message is concatenated to the signaling parts of the packet including the training sequence with the start and end flags of the message. Next, it is encoded through non-return to zero inverted (NRZI) and modulated with GMSK as described hereinafter.

C. Transmission Signal Model

AIS signals transmit data using the GMSK modulation [19], a particular form of continuous phase modulation (CPM) that we describe in details in this section. We consider a sequence of N independent and identically distributed (i.i.d.) symbols $\mathbf{a} = \{a_i\}_{0 \leq i \leq N-1}$ to be transmitted such that $a_i \in \mathcal{M} = \{\pm 1\}$. Let $s(t, \mathbf{a})$ denote the complex envelope of the AIS signal given by

$$s(t, \mathbf{a}) = \sqrt{\frac{2E_s}{T_s}} e^{j\theta(t, \mathbf{a})} \quad (1)$$

where E_s is the average symbol energy, T_s is the symbol duration. $\theta(t, \mathbf{a})$ is the signal phase that depends on the symbol sequence \mathbf{a} , defined by:

$$\theta(t, \mathbf{a}) = 2\pi h \sum_{i=0}^{N-1} a_i q(t - iT_s) \quad (2)$$

with h the modulation index and $q(t)$ the phase shaping pulse. In practice, the infinite GMSK frequency pulse support is truncated to $[0, LT_s]$ and referred to as L -GMSK where L is the CPM memory.

D. Received Signal Model

In this paper, it is assumed that the satellite is equipped with just one antenna for reception, and that each vessel has one antenna for transmitting the AIS signals. A slowly varying channel during each AIS signal transmission with pure line of sight (LOS) path is considered. Furthermore, perfect acquisition of signals is assumed and we denote by "detection" the process of estimating data symbols in received AIS signals. The multi-user received signal model during a given AIS time slot can be written in a complex baseband representation as

$$r(t) = \sum_{i=1}^{\mathcal{N}} \alpha_i s_i(t - \tau_i, \mathbf{a}) e^{j(2\pi f_{d,i}(t) + \phi_i)} + n(t) \quad (3)$$

where \mathcal{N} is the number of colliding AIS signals, $s_i(t, \mathbf{a})$ is the i^{th} AIS signal with $1 \leq i \leq \mathcal{N}$, α_i is the attenuation coefficient of the LOS path, τ_i is the propagation delay, ϕ_i is the phase shift of the i^{th} path and is uniformly distributed in $[0, 2\pi)$. $f_{d,i}(t)$ is defined as $f_{d,i}(t) = f_{d,i} + \eta_i t/2$, it represents the time varying Doppler frequency shift associated with the i^{th} signal with $f_{d,i}$ as the initial Doppler shift and η_i standing for the Doppler rate of the signal. $n(t)$ is a complex circular stationary AWGN noise with single-sided power spectral density $2N_0$.

We assume that for a given user of interest, the receiver has a perfect knowledge of these propagation parameters with perfect carrier frequency and timing synchronization. We neglect the effect of Doppler rate ($\eta_i = 0$) having limited impact due to the sufficiently slow frequency variation compared to the AIS message duration, in this case $f_{d,i}(t) = f_{d,i}$.

III. DETECTION FOR SPACE-BASED AIS

A. Maximum Likelihood Sequence Estimation Principle

The decoding algorithm is described for an AWGN channel model. It will be applied in the multiple access system model when the receiver is perfectly synchronized with the signal of interest and the multiple access interference is considered as an additional noise. In the single-user AWGN channel model, the described coherent detection is optimal. The equivalent baseband received signal is given by:

$$r(t) = s(t - \tau, \mathbf{a})e^{j(2\pi f_d t + \phi)} + n(t) \quad (4)$$

with f_d , τ , ϕ and $n(t)$ having the same definition as in (3). The MLSE algorithm maximizes the correlation between $r(t)$ and $s(t, \hat{\mathbf{a}})$ over all possible realizations for $\hat{\mathbf{a}}$.

$$\hat{\mathbf{a}} = \arg \max_{\hat{\mathbf{a}}} \Re \left[\int r(t) s^*(t - \tau, \hat{\mathbf{a}}) e^{-j(2\pi f_d t + \phi)} dt \right] \quad (5)$$

where $(\cdot)^*$ is the complex conjugate and \Re represents the real part.

B. Coherent MLSE-Detector of CPM

In coherent detection, channel parameters need to be estimated by the receiver. In practice, it requires a preliminary synchronization step.

To solve the complexity problem involved by the computation of the different correlation metrics, the Viterbi algorithm [18] is applied using the trellis representation of the CPM.

The phase of the baseband CPM signal in (2) can be split into two main terms as follows:

$$\begin{aligned} \theta(t, \mathbf{a}) &= 2\pi h \sum_{i=n-L+1}^n a_i q(t - iT_s) + \pi h \sum_{i=0}^{n-L} a_i \\ &= \Theta_n(t) + \theta_n \end{aligned} \quad (6)$$

The first term $\Theta_n(t)$ corresponds to the contribution of the current and last $(L-1)$ symbols, θ_n describes the contribution

of the rest of the past symbols. For the optimal coherent detector, the trellis states are represented by the phase evolution and the previous $(L-1)$ symbols given by the state vector:

$$\sigma(n) = [\theta_n, a_{n-L+1}, \dots, a_{n-1}] \quad (7)$$

Let $h = u/p$ where u and p are co-prime integers. The number of states is equal to $S = pM^{L-1}$ or $S = 2pM^{L-1}$ if u is even or odd respectively.

Given the state σ_i at instant $n+1$, the Viterbi algorithm computes the cumulative metric for each possible transition towards this state. Then it selects and stores the previous state which yields the maximum one.

$$\Lambda_{n+1}(\sigma_i) = \max_{\sigma_j \rightarrow \sigma_i} \{\Lambda_n(\sigma_j) + \delta_n(\sigma_j, \sigma_i)\} \quad (8)$$

where $\delta_n(\sigma_j, \sigma_i)$ denotes the branch metric from state σ_j to state σ_i with i and $j \in \llbracket 1, S \rrbracket$ and is defined as

$$\delta_n(\sigma_j, \sigma_i) = \Re \left[\int_{nT_s}^{(n+1)T_s} r(t) s^*(t - \tau, \hat{\mathbf{a}}) e^{-j(2\pi f_d t + \phi)} dt \right] \quad (9)$$

At the end, the MLSE-based decision is taken by selecting the final state with highest cumulative metric. A backtracking is applied to deliver the corresponding estimated symbol sequence $\hat{\mathbf{a}}$.

C. Optimized Differential MLSE-Detector

Using a differential detector [20] [21], the phase of the incoming signal is tracked based on the phase difference between consecutive symbols. The received signal is multiplied by a time-delayed and conjugate version of itself, thus this process simplifies the detection problem by eliminating the phase shift ϕ coming from the transmission. Let K be the delay factor. The differential signal is given by:

$$R_K(t) = r(t)r^*(t - KT_s) = S_K(t - \tau, \mathbf{a})e^{j(2\pi f_d KT_s)} + N_K(t) \quad (10)$$

with $r(t)$ defined as in (4), $N_K(t)$ depending on both the signal and the AWGN noise [21], and S_K defined as:

$$S_K(t, \mathbf{a}) = \frac{2E_s}{T_s} e^{i(\Theta_K(t, \mathbf{a}))}, \quad (11)$$

where $\Theta_K(t, \mathbf{a}) = \theta(t, \mathbf{a}) - \theta(t - KT_s, \mathbf{a})$. With $0 \leq \zeta < T_s$, the differential phase $\Theta_K(\zeta + nT_s, \mathbf{a})$ reads:

$$\begin{aligned} \Theta_K(\zeta + nT_s, \mathbf{a}) &= \varphi_n(\zeta) + \theta_n \\ \text{with } \varphi_n(\zeta) &= 2\pi h \sum_{i=0}^{L-1} (a_{n-i} - a_{n-K-i}) q(\zeta + iT_s) \\ \text{and } \theta_n &= \pi h \sum_{i=0}^{K-1} a_{n-L-i} \end{aligned} \quad (12)$$

These two terms $\varphi_n(\zeta)$ and θ_n are fully determined by the set of symbols a_{n-i} with $1 \leq i < L + K - 1$. Thus unlike the trellis of the original CPM signal, in this case θ_n does not

need to be stored as a state parameter. The state is defined as $\Sigma(n) = [a_{n-L-K+1}, \dots, a_{n-1}]$ with M^{K+L-1} different possible states independent from the modulation index. The MLSE detection criterion described in Section III-A applies on the resulting differential signal replacing r and s by R_k , S_K in (5). The differential detector has been proven to be efficient for GMSK and $L = 3$ with the optimized delay value $K = 3$ [21].

IV. PARALLEL LIST VITERBI ALGORITHM FOR AIS SIGNAL DECODING

To improve the detection of the AIS signals by increasing the diversity of candidates, we propose to use the LVA, taking advantage of the CRC embedded in the AIS message. We describe in this section the principle of "Parallel LVA" [11], [12] and its implementation details.

A. Principle

PLVA is an extension of the traditional Viterbi algorithm, it ensures the diversity of candidates by maintaining a list of multiple paths with their corresponding metrics instead of only keeping the most likely path. Two main parameters could be considered for PLVA: P The number of paths stored for each state at each stage of the trellis, and C the number of the most likely candidates chosen at the final stage of the trellis.

PLVA produces an ordered list of the best estimates of the transmitted information sequence following the trellis search, this requires computing the P best paths for each state at every trellis section.

B. Algorithm

For S states, N transmitted symbols and P paths, PLVA requires maintaining a cumulative metric array of the P maximum cumulative metrics and a state array which stores their path history (the previous state and the rank of the previous path) for each time instant in the trellis. For a state σ_i at instant n , a list sorted in decreasing order of size P is stored. This list contains the P maximum cumulative metrics of the P paths reaching σ_i state. This is illustrated in Fig. 2. The path with the highest cumulative metric is considered to be the most likely path, the path with the second highest cumulative metric is considered to be the second most likely path and so on.

The cumulative metric of the k -th most likely path reaching state σ_i at instant n is denoted by $\Lambda_n(\sigma_i, k)$. For $n = 0$, decoding starts from a state with only one cumulative metric initialized such that $\Lambda_0(\sigma_i, 1) = 0$. At instant $n + 1$, the length- P cumulative metric vector for state σ_i denoted by $\Lambda_{n+1}(\sigma_i) = [\Lambda_{n+1}(\sigma_i, 1), \Lambda_{n+1}(\sigma_i, 2), \dots, \Lambda_{n+1}(\sigma_i, P)]^T$ where $(\cdot)^T$ stands for transposition, is computed as follows:

$$\Lambda_{n+1}(\sigma_i) = \max_{\substack{(P) \\ \sigma_j \rightarrow \sigma_i \\ k \in [1, P]}} (\{\Lambda_n(\sigma_j, k) + \delta_n(\sigma_j, \sigma_i)\}) \quad (13)$$

with $\max^{(P)}(\mathcal{S})$ denoting the function that selects the P highest values in the set \mathcal{S} .

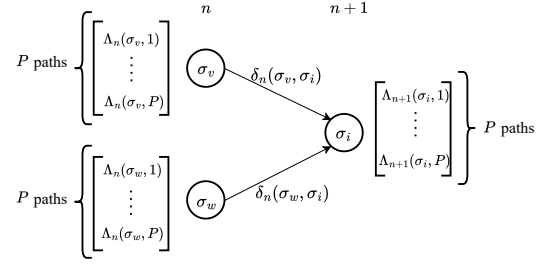


Fig. 2: Cumulative Metrics of the PLVA

At the last (N -th) trellis section, C candidates with the highest cumulative metrics among the SP paths stored in the lists of final states are extracted. The PLVA decoding is followed by the post processing by which the NRZI decoding is applied followed by two main criteria for selecting the right candidate. After the stuffing bits retrieval, the length criterion is applied on the decoded frame making sure whether it is equal to 184, which is the length of the AIS data message. If this is not the case, the frame is discarded. Otherwise, if the length condition is satisfied, the selected frame undergoes the CRC check criterion.

To reduce processing time without affecting performance, a stop criterion can be applied. Candidates are ranked in descending order according to their cumulative metric. When one of them satisfies all the constraints mentioned above (length-184, valid CRC), it is selected as the decision and the post-processing stops. If none of the candidates meet the two post-processing criteria, an error is declared and no signal is detected.

For small list sizes, the complexity of the PLVA is generally considered acceptable when compared to that of the classical Viterbi Algorithm. Whenever the complexity is critical, several implementations of the LVA are presented in [17] including PLVA, SLVA and its improved versions. With any of these implementations a similar performance could be attained when the list size P is properly tuned. Despite the slightly higher complexity of PLVA, its parallel nature makes it a more straightforward and easier-to-implement option with reduced decoding latency, which is why it is often chosen in practice.

V. NUMERICAL RESULTS

In this section, we compare the performance in terms of AIS message recovery of the receiver based on the PLVA with the one based on the VA applied either on the original or the differential received signal. The generic system model is given in (3) and we assume perfect channel parameter knowledge at the receiver. We first consider the single user AWGN channel in Section V-A. Then we optimize the parameters (P, C) of the PLVA based on a simplified two-user AIS channel. In the last part, we evaluate the performance in a more realistic AIS multiple-access scheme with low-to-high system load. According to AIS signal definition, in the simulation setup we

take symbol period $T_s = 1/9600s$, $BT = 0.4$, CPM memory $L = 3$ and modulation index $h = 0.5$.

A. Detection in a single-user AWGN channel

We first illustrate the influence of the list parameters (P, C) on the PLVA detection performance of AIS messages in a single-user AWGN channel. For that we simulated the PLVA with the coherent detector given P equals $\{1, 16, 2048\}$ and optimized differential detector given P equals $\{1, 16\}$ and $C = P$. The packet error rate (PER) is plotted as a function of E_b/N_0 in Fig. 3. The curve corresponding to the differential detector ($k = 1$) with VA ($P = 1$) serves as an upper bound on the error rate. We observe that with PLVA having $P = 16$ the coherent detector performance improved by approximately 3 dB compared to the VA ($P = 1$) at $PER = 10^{-3}$. Similarly for the optimized differential detector, with $P = 16$, a gain of $\simeq 2$ dB compared to VA ($P = 1$) is obtained. Thus, the data error rate is reduced with the increase of list size for both the coherent and optimized differential detectors. Hence, PLVA shows remarkable improvement of the performance compared to VA in the single-user scenario, especially given the limited computational complexity increase of the LVA with respect to the classical VA approach.

We have also plotted the performance of two other state-of-the-art AIS receivers: the receiver depicted in [6] whose complexity is prohibited for practical applications but which achieves the best performance to the best of our knowledge and the receiver described in [5] but assuming perfect synchronization contrary to the work of [5] where synchronization is implemented. We observe that the PLVA with $(P, C) = (16, 16)$ outperforms [5] by approximately 1 dB at a PER of 10^{-4} and that the PLVA with $(P, C) = (2048, 2048)$ approaches the lower bound given by [6], converging beyond 6 dB ($PER \downarrow 10^{-4}$). In the next section, we show that optimizing C with fixed P further improves the performance in most cases. With $(P, C) = (2048, 4096)$, the additional gain is negligible, indicating that the best achievable performance with the PLVA is reached at $P = 2048$ and $C \geq 2048$.

B. Optimization of parameters (P, C) of the PLVA

In order to optimize the parameters (P, C) of PLVA, we assume having two interfering signals. Focusing on one transmitted signal of interest at a time, and assuming we have only a single interferer with the overlap equal to $\{17\%, 83\%$ of the actual data (data, CRC bits and stuffed bits) approximately corresponding to the worst case scenario of the Class 2 Interference and the best case scenario of the Class 1 Interference considering a representative Sat-AIS scenario. The receiver synchronizes itself with respect to the strongest-received power signal.

The PLVA performance depends on the parameters (P, C) . Therefore the optimization of these parameters is a must to meet a trade-off between performance and complexity. The optimized P and C values for both the coherent and differential detectors in a two-user channel model are provided in Table I, assuming a -3 dB power difference, $\{17\%, 83\%$

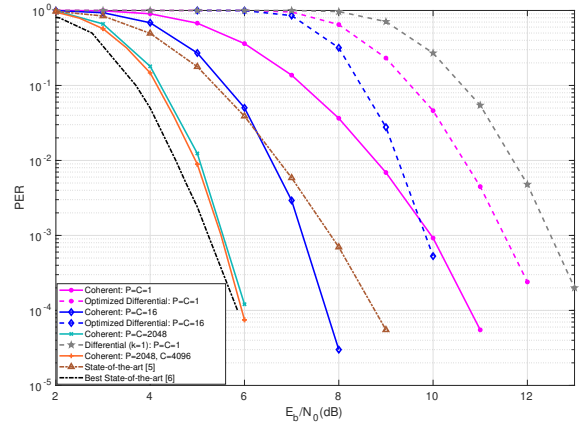


Fig. 3: Effect of PLVA application with the coherent and optimized differential detectors on the probability of detection in a single-user AWGN channel with varying (P, C) values compared to two state-of-the-art AIS coherent receivers [5], [6].

TABLE I: Optimized PLVA parameters for AIS signal detection in a Two-user multiple access channel - Target PER of -3 dB power difference and $\{17\%, 83\%$ overlap

	List size P	Number of candidates C
Coherent detector	64	256
Optimized Differential detector	128	512

overlap and neglected Doppler shift difference. The optimized values of P and C remain consistent regardless of whether the overlap is minor or major. For the coherent detector with PLVA, taking $(P, C) = (64, 256)$ enables to achieve the same performance gain as $(P, C) = (256, 256)$ with reduction of storage requirement and of processing complexity and time. The same applies for the optimized differential decoder for $(P, C) = (128, 512)$ showing a gain similar to that obtained by $(P, C) = (512, 512)$.

C. System-level Simulations

In this subsection, we consider a more realistic AIS reception scenario from a LEO satellite to provide insights onto the overall reception performance. The satellite altitude is chosen equal to 656.5 km and the AIS transmitting vessels are uniformly distributed in the satellite swath (up to 0 degree ground elevation). For simplicity, the access protocol is modeled under a slotted ALOHA hypothesis (local SOTDMA organization is neglected). This approximation is relevant considering that the satellite swath is much larger than an SOTDMA-organized area and was already considered as a surrogate model for the satellite-AIS reception in [22]. A number of arrivals per AIS frame is set and the slot choice for each signal is independent and uniformly distributed. The received C/N_0 , propagation delays and Doppler characteristics are computed assuming static emitters and a simple yet sufficiently representative link

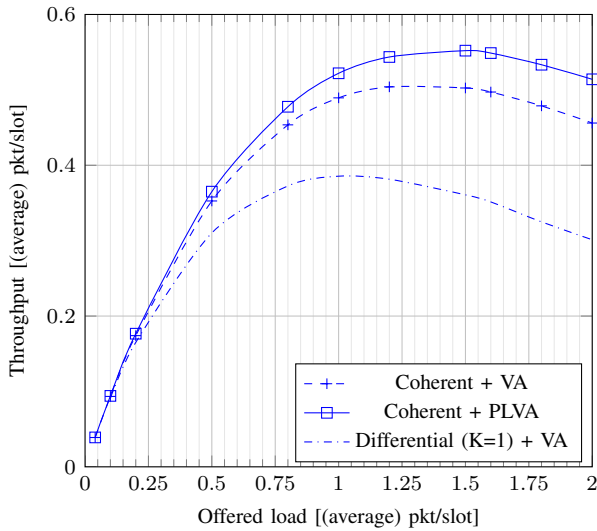


Fig. 4: Throughput as a function of the offered load, considering Coherent detection using the VA and PLVA with $(P, C) = (64, 256)$ and usual Differential detection with $K = 1$ using the VA taken as a lower bound.

budget assuming a pure LOS path (without fading, hence resulting in a limited dispersion of E_s/N_0 among users).

Considering coherent receivers, the system throughput of the VA and PLVA (with $P, C = (64, 256)$) is depicted in Fig. 4 with the usual differential detector ($K = 1$) curve with VA taken as a lower bound. PLVA significantly outperforms the differential detector used before for AIS. Comparing the two coherent detectors, it can be shown that the PLVA allows an increase in maximum throughput of ≈ 0.05 (average) pkt/slot and increases the throughput at high system loads, without the use of any interference cancellation strategy. This gain is expected to be even greater with a SIC scheme.

VI. CONCLUSION

In this article, we propose the application of the Parallel-List Viterbi algorithm (PLVA) for the purpose of improving the success rate of correct detection of the AIS messages. The performance of PLVA with optimized parameters is studied with the coherent and optimized differential detectors for the decoding of AIS signals. Simulations of the AIS detection in a single user AWGN channel show that the performance of the proposed algorithm is much improved compared to the Viterbi algorithm with the best results exceeding the performance in [5] and approaching the lower bound given by [6], thus showing the effectiveness of PLVA. Finally, simulations under realistic collision conditions with varying channel overload with optimized PLVA is addressed, which leads to promising perspectives concerning the application of PLVA to improve the primary detection step in SIC algorithms.

REFERENCES

[1] Recommendation ITU-R M1371-5, *Technical characteristics for an automatic identification system using time-division multiple access in the*

VHF maritime mobile band. International Telecommunication Union, 2014.

[2] M. A. Cervera, A. Ginesi, and K. Eckstein, "Satellite-based vessel automatic identification system: A feasibility and performance analysis," *International Journal of Satellite Communications and Networking*, vol. 29, no. 2, pp. 117–142, 2011.

[3] M. Zhou, A.-J. van der Veen, and R. van Leuken, "Multi-user leo-satellite receiver for robust space detection of ais messages," in *2012 IEEE ICASSP*, 2012, pp. 2529–2532.

[4] M. Picard, M. R. Oularbi, G. Flandin, and S. Houcke, "An adaptive multi-user multi-antenna receiver for satellite-based AIS detection," in *2012 6th ASMS Conference and 12th SPSC Workshop*, 2012, pp. 273–280.

[5] G. Colavolpe, T. Foggi, A. Ugolini, J. Lizarraga, S. Cioni, and A. Ginesi, "A highly efficient receiver for satellite-based automatic identification system signal detection," in *2014 7th ASMS Conference and 13th SPSC Workshop*, 2014, pp. 120–127.

[6] R. Prévost, M. Coulon, D. Bonacci, J. LeMaitre, J.-P. Millerioux, and J.-Y. Tourneret, "Cyclic redundancy check-based detection algorithms for automatic identification system signals received by satellite," *International Journal of Satellite Communications and Networking*, vol. 31, no. 3, pp. 157–176, 2013.

[7] Y. Takanezawa, Y. Chang, K. Fukawa, and D. Hirahara, "Separate detection of collided packets using parallel interference cancellation over space-based AIS channels," *IEICE Technical Report*, vol. 119, no. 417, p. 33–38, 2020.

[8] S. Uehashi, Y. Nouda, M. Hangai, and T. Ohgane, "Successive interference cancellation for asynchronous signal collision in space-based ais," in *2022 IEEE Aerospace Conference*, 2022, pp. 1–7.

[9] A. Hassanin, F. Lázaro, and S. Plass, "An advanced ais receiver using a priori information," in *OCEANS 2015 - Genova*, 2015, pp. 1–7.

[10] F. Clazzer, F. Lázaro, and S. Plass, "New receiver algorithms for satellite ais," in *Deutscher Luft- und Raumfahrtkongress*, 09 2015.

[11] N. Seshadri and C.-E. Sundberg, "List Viterbi decoding algorithms with applications," *IEEE Transactions on Communications*, vol. 42, no. 234, pp. 313–323, 1994.

[12] N. Seshadri and C.-W. Sundberg, "Generalized Viterbi algorithms for error detection with convolutional codes," in *1989 IEEE Global Telecommunications Conference and Exhibition 'Communications Technology for the 1990s and Beyond'*, 1989, pp. 1534–1538 vol.3.

[13] C. Nill and C.-E. Sundberg, "List and soft symbol output Viterbi algorithms: extensions and comparisons," *IEEE Transactions on Communications*, vol. 43, no. 2/3/4, pp. 277–287, 1995.

[14] S. Manji and G. Djuknic, "Bandwidth efficient and error resilient image coding for rayleigh fading channels," in *1999 IEEE 49th Vehicular Technology Conference*, vol. 2, 1999, pp. 1485–1489 vol.2.

[15] V. Sánchez and A. M. Peinado, "An efficient parallel algorithm for list Viterbi decoding," *Signal Processing*, vol. 83, no. 3, pp. 511–515, 2003.

[16] H. Yang, E. Liang, and R. D. Wesel, "Joint design of convolutional code and CRC under serial list viterbi decoding," *CoRR*, vol. abs/1811.11932, 2018. [Online]. Available: <http://arxiv.org/abs/1811.11932>

[17] H. Yang, S. V. S. Ranganathan, and R. D. Wesel, "Serial list Viterbi decoding with CRC: Managing errors, erasures, and complexity," in *2018 IEEE Global Communications Conference*, 2018, pp. 1–6.

[18] G. D. Forney, "The Viterbi algorithm," *Proceedings of the IEEE*, vol. 61, no. 3, pp. 268–278, 1973.

[19] J. B. Anderson, T. Aulin, and C.-E. W. Sundberg, "Digital phase modulation," in *Applications of Communications Theory*, 1986. [Online]. Available: <https://api.semanticscholar.org/CorpusID:107067311>

[20] M. Simon and C. Wang, "Differential versus limiter - discriminator detection of narrow-band FM," *IEEE Transactions on Communications*, vol. 31, no. 11, pp. 1227–1234, 1983.

[21] A. Jerbi, K. Amis, F. Guilloud, and T. Benaddi, "Delay optimization of conventional non-coherent differential CPM detection," *IEEE Communications Letters*, vol. 27, no. 1, pp. 234–238, 2023.

[22] F. Clazzer and A. Munari, "Analysis of capture and multi-packet reception on the AIS satellite system," in *OCEANS 2015 - Genova*, 2015, pp. 1–9.